Int. J. Electrochem. Sci., 9 **(2014)** 5560 - 5573

International Journal of
ELECTROCHEMICAL
SCIENCE
www.electrochemsci.org

Corrosion Inhibition of Al-alloy in 3.5% NaCl Solution by a Natural Inhibitor: An Electrochemical and Surface Study

Wanying Liu[1], *Ambrish Singh*[1,2], *Yuanhua Lin*[1,*], *Eno. E. Ebenso*[3,4], *Guan Tianhan*[1], *Chengqiang Ren*[5]

[1] State Key Laboratory of Oil and Gas Reservoir Geology and Exploitation (Southwest Petroleum University), Chengdu, Sichuan 610500, China.
[2] Department of Chemistry, School of Civil Engineering, LFTS, Lovely Professional University, Phagwara, Punjab, India.
[3]Department of Chemistry, School of Mathematical & Physical Sciences, North-West University(Mafikeng Campus), Private Bag X2046, Mmabatho 2735, South Africa.
[4] Material Science Innovation & Modelling (MaSIM) Focus Area, Faculty of Agriculture, Science and Technology, North-West University (Mafikeng Campus), Private Bag X2046, Mmabatho 2735, South Africa.
[5] School of Material Science and Engineering (Southwest Petroleum University), Chengdu, Sichuan 610500, China.
[*]E-mail: yhlin28@163.com

Received: 22 February 2014 / *Accepted:* 4 April 2014 / *Published:* 16 July 2014

Root extract of *Coptis chinensis* (CCR) was used and its inhibition efficiency on corrosion of Al alloy in 3.5 wt.% NaCl was investigated through surface morphology and electrochemical techniques. The Nyquist diagrams containing the extract with different concentrations showed increase in R_{ct} values, thus increasing inhibition efficiency. Potentiodynamic curves suggested that the extract acted as mixed type in nature. The surface analysis through scanning electrochemical microscopy (SECM), UV-Visible Spectroscopy for Al alloy specimens also proved the results obtained by the electrochemical experiments. The adsorption of the studied inhibitor obeyed the Temkin's adsorption isotherm.

Keywords: Aluminium; EIS, Polarization; FTIR Spectroscopy; Coptis chinensis

1. INTRODUCTION

Corrosion is defined as the deterioration of a material, usually a metal, because of its reaction with the environment [1]. Because of their high strength-to-density ratio, the wrought aluminum–zinc–magnesium–copper AA7075 series alloys are commonly used in the transport applications, including marine, automotive and aviation industry. Rock climbing equipment, bicycle components,

inline skating-frames, and hang glider airframes are commonly made from 7075 aluminium alloy. Hobby grade RC models commonly use 7075 for chassis plates. One interesting use for 7075 is in the manufacture of M16 rifles for the American military. Due to its strength, high density, thermal properties, and its ability to be highly polished, 7075 is widely used in mold tool manufacture. 7075 aluminium alloy is strong, with strength comparable to many steels, and has good fatigue strength and average machinability [2, 3].

Aluminum has a natural corrosion protection from its oxide layer, but if exposed to aggressive environments, it may corrode. Especially in the presence of chloride ions (Cl^-), such as in seawater, the oxide is broken down. 7075 aluminium series alloys are susceptible to local corrosion caused by the presence of an intermetallic phase in their structure [4, 5].

Corrosion inhibitors are widely used in industry to reduce the corrosion rate of metals and alloys that are present in contact with aggressive environments. The protective film occurs on the metal surface with a mechanism of adsorption of inhibitors to avoid metals from corrosion, so the surface of the metal and the inhibitor interact with each other. There are two types of corrosion inhibitors: inorganic and organic. The protective action of inorganic inhibitors is related to the formation of oxide film or hardly soluble salt on the metal surface. On the other hand, the protective action of organic inhibitors comes from the adsorption on the oxide films. Compounds having heteroatoms, such as oxygen, sulfur, and nitrogen, and heterocyclic compounds containing functional groups and conjugated double bonds can be used as corrosion inhibitors [6].

The most common inorganic inhibitors used for Al or Al alloys are chromates [7]. At the same time, because of the environmental legislations and high toxicity of chromate and organic phosphate, there is a considerable interest in their replacement. Despite the large number of organic compounds, there is always a need for the development of new corrosion inhibitors. Because of increasing ecological awareness and strict environmental regulations, as well as the inevitable drive toward sustainable and environmentally benign processes, attention now has been focused toward the development of nontoxic alternatives to inorganic and organic inhibitors applied so far [8]. There have been many research reports on natural products as corrosion inhibitors in different aggressive environments [9-13].

Coptis chinensis, the Chinese goldthread, is a species of goldthread native to China. *Coptis chinensis* is one of the 50 fundamental herbs used in traditional Chinese medicine, where it is called *duăn è huánglián* in Chinese. The rhizomes of *Coptis chinensis* are used in Traditional Chinese Medicine and serve as a source for the isoquinoline alkaloids berberine, palmatine, hydrastinine and coptisine [14]. A study in rats suggested berberine (the primary alkaloid in *Coptis*) is potential agents for preventing intestinal injury [15]. Because of the strong coloring quality of berberine (5,6-dihydro-9,10-dimethoxybenzo[g]-1,3-benzodioxolo[5,6-a]quinolizinium) as in figure 1, slowly soluble in water, yellow in appearance and melting point of 145^{o}C, it has been traditionally used as a dye, especially for wool and other fibers. It is the only cationic dye among the natural plant dyes that is part of the chemical group of isoquinoline alkaloids [16]. In present work we elucidated the inhibition effect of *Coptis chinensis* root extract on corrosion of 7075 aluminium alloy in 3.5% NaCl using electrochemical impedance spectroscopy (EIS), potentiodynamic polarization techniques, scanning electrochemical microscopy (SECM), and UV-Visible spectroscopy.

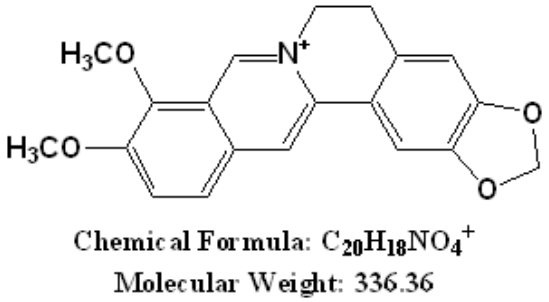

Figure 1. CCR extract active constituent Berberine- IUPAC name (5,6-dihydro-9,10-dimethoxybenzo[g]-1,3-benzodioxolo[5,6-a]quinolizinium).

2. EXPERIMENTAL

2.1. Preparation of Inhibitor

Fifty grams of dried *Coptis chinensis* plant roots were soaked in 900 ml of reagent grade ethanol for 24 h and refluxed for 5 h. The ethanolic solution was vacuum dried. The yellow powder obtained was refluxed with 3.5% NaCl solution for 5 hours. This solution was concentrated to 500 ml. This solution was used to study the corrosion inhibition properties.

2.1.1. Fourier Transform Infra Red Spectroscopy (FTIR)

FT-IR spectra (KBr) in transmittance mode were recorded on a Nicolet-6700 spectrophotometer. The peaks obtained as in figure 2 are 482.15 -Br group; 606.59 C-H bending; 863.77 C-N stretching; 934.28 –OH group; 984.06 C-O bending; 1100.20 C-O stretching; 1390.56 C=C (Aromatic); 1618.70 C=C (Aromatic); 1726.55 C=O stretching; 3232.26 N-H stretching; 3418.92 –OH groups; 3476.99 OH-NH stretching vibration; 3555.81 –OH groups.

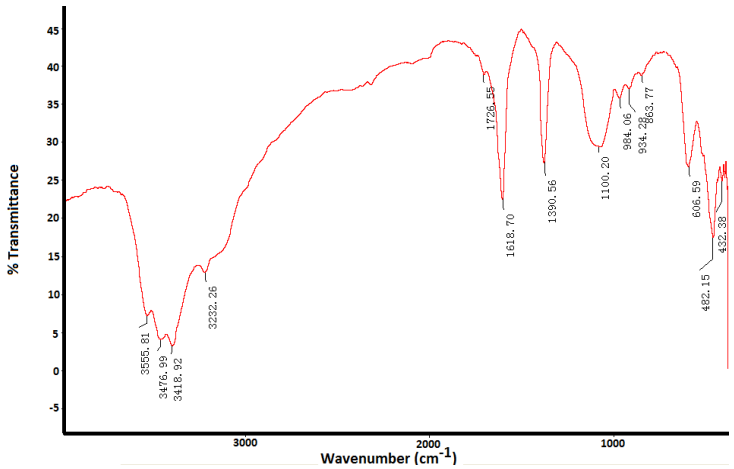

Figure 2. FT-IR transmittance spectra of *Coptis chinensis* root extract.

2.1.2. Gas Chromatography (GC) Analysis

GC analyses were carried out using a GC-2010 Plus, (Shimadzu Japan) GC apparatus equipped with a single injector and two flame ionization detectors (FID). The apparatus was used for simultaneous sampling to two fused-silica capillary columns (60 m × 0.22 mm, film thickness 0.25 μm) with different stationary phases: (polydimethylsiloxane) and (polyethylene glycol). Temperature program: the oven temperature was programmed from 60°C to 200°C and then held isothermally at 200 °C (20 min).

Carrier gas used in the process was He (1 mL/min). Injector and detector temperatures were held at 200 °C. Split injection was conducted with a ratio split of 1:50. Relative component concentrations were calculated based on GC peak areas without using correction factors. A number of prominent peaks as shown in were identified in the repeated GC analyses of the CCR extract and the result is shown in figure 3. Among the peaks identified, they are very similar to alkaloids and close to GC of berberine [17].

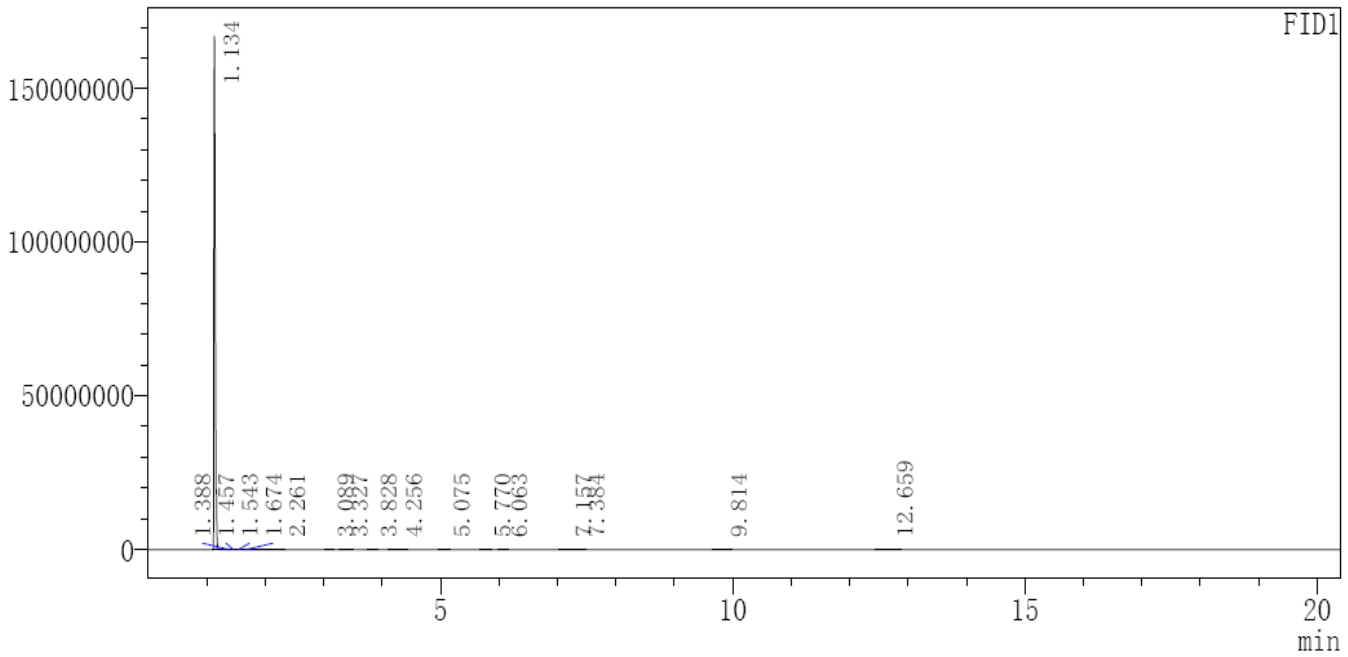

Figure 3. GC analysis of *Coptis chinensis* root extract.

2.2. Materials and Solutions

Aluminium 7075 alloy with density 2.83 g/cm^3 having following composition (wt %): Si 0.41; Cu 1.38; Mg 2.62; Zn 5.89; Mn ≤ 0.30; Ti ≤ 0.20; Fe 0.50 and balance Al were used for all studies. Aluminium alloy coupons having dimensions of 30 mm × 3 mm × 3 mm were used for the electrochemical study. The specimens were metallographically polished according to ASTM A262,

degreased, and dried before experiment. The test solution of 3.5% NaCl was prepared by analytical grade NaCl with double distilled water.

2.3. Electrochemical measurements

The electrochemical experiments were performed by using three electrode cell, connected to Potentiostat/Galvanostat CHI604D. Zview software package was used for data fitting. Aluminium alloy was used as working electrode, platinum electrode as an auxiliary electrode, and saturated calomel electrode (SCE) as reference electrode. All potentials reported were measured versus SCE. Tafel curves were obtained at a scan rate of 1.0 mVs^{-1}. EIS measurements were performed under potentiostatic conditions in a frequency range from 100 kHz to 0.01 Hz, with amplitude of 10 mV AC signal. The experiments were carried out when the electrochemical system was in steady state in 3.5% NaCl in absence and presence of different concentrations of CCR extract. All experiments were carried out at room temperature in unstirred solutions.

2.4. Surface Morphological Studies

2.4.1. Scanning Electrochemical Microscopy (SECM)

Scanning electrochemical microscopy (SECM) is a technique in which the current that flows through a very small electrode tip (generally an ultramicroelectrode with a tip diameter of 10 pm or less) near a conductive, semiconductive, or insulating substrate immersed in solution is used to characterize processes and structural features at the substrate as the tip is moved near the surface [18-20]. The tip can be moved normal to the surface (the *z* direction) to probe the diffusion layer, or the tip can be scanned at constant *z* across the surface (the *x* and *y* directions). The tip and substrate are part of an electrochemical cell that usually also contains other (e.g., auxiliary and reference) electrodes. The diameter of the samples was between 30 × 3 × 3 mm. A model of scanning electrochemical microscopy CHI900C was used. The instrument was operated with a 10 μm platinum tip as the probe, an Ag/AgCl/KCl (saturated) reference electrode, and a platinum counter electrode. All potential values are referred to the Ag/AgCl/KCl (saturated) reference electrode. The measurements of line scans were generated with the tip at ~ 10 μm from the specimen surface in all the cases. The scan rate was 80 μm/step.

2.4.2. UV-Visible Spectroscopy

UV-Visible absorption spectra were measured with UV-5100 double beam spectrophotometer. The CCR extract solution (1000 ppm) and the washing solution obtained after 3 hrs of immersion of aluminium alloy were subjected to UV-Visible absorption detection.

3. RESULTS AND DISCUSSION

3.1. Electrochemical measurements

3.1.1. Potentiodynamic polarization measurements

The model we use for corrosion process assumes that the rates of both the anodic and cathodic processes are controlled by the kinetics of the electron transfer reaction at the metal surface. This is generally the case for corrosion reactions.The corrosion potential (E_{corr}), corrosion current density (I_{corr}), and anodic (β_a) and cathodic (β_C) slopes are obtained by the anodic and cathodic regions of the tafel plots shown in table 1.

Table 1. Polarisation parameters and inhibition efficiency values for aluminium alloy in 3.5% NaCl in absence and presence of CCR extract.

Inhibitor	Conc.(ppm)	Tafel data				
		E_{corr} (V vs. SCE)	I_{corr} (μA cm^{-2})	b_a (mV d^{-1})	b_c (mV d^{-1})	η (%)
3.5% NaCl	-	-1.2	52	106	163	-
CCR Extract	250 ppm	-1.2	35	65	108	32
	500 ppm	-1.3	11	34	111	79
	1000 ppm	-1.3	03	72	34	94

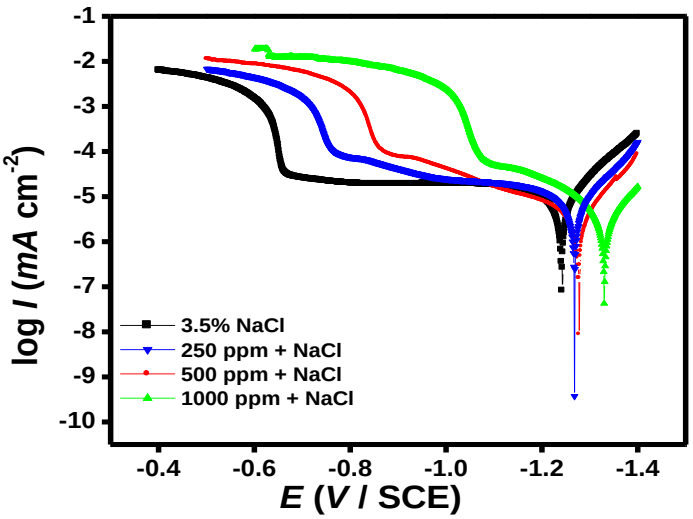

Figure 4. Tafel plots for aluminium alloy in 3.5% NaCl without and with optimum concentrations of CCR extract.

The results showed the decrease in I_{corr} in presence of inhibitor as compared to blank solution this is due to adsorption of inhibitor on metal surface which penetrates rate of corrosion current density and increases inhibition efficiency [21-23]. The corrosion current density (I_{corr}) can be obtained by

extrapolating the tafel lines to the corrosion potential and the inhibition efficiency (η %) values were calculated from the relation:

$$\eta\% = \frac{I_{corr} - I_{corr(i)}}{I_{corr}} \times 100 \quad (1)$$

where, I_{corr} and $I_{corr(i)}$ are the corrosion current density in absence and presence of inhibitor. The polarization curves for aluminium alloy in the absence and presence of inhibitors are given in figure 4.

Figure 4 also illustrates the movement of curves towards the passive and transpassive regions which are common in aluminium alloys [24-28]. The inhibitor is more predominant towards the cathode with respect to anode as is evident from the figure.

3.1.2. Electrochemical Impedance Spectroscopy

Electrochemical impedance spectroscopy measurements were carried out in order to study the kinetics of the electrode process and the surface properties of the studied system. This method is widely used to investigate the corrosion inhibition process [29, 30]. Nyquist plots of aluminium alloy in 3.5% NaCl solution in the absence and presence of different concentrations of CCR extract are shown in figure 5. A high frequency depressed charge transfer semicircle is observed [31, 32]. It is clear from figure 5 that the impedance spectra are not perfect semicircles and the depressed capacitive loop corresponds to surface heterogeneity which may be the result of surface roughness, dislocation, distribution of active sites, or adsorption of the different CCR extract molecules [33-36].

The model used for fitting consist the solution resistance (R_s), the charge-transfer resistance of the interfacial corrosion reaction (R_{ct}) and the constant phase angle element (CPE).

The inhibition efficiency is calculated using charge transfer resistance (R_{ct}) as follows,

$$\eta\% = \frac{R_{ct(inh)} - R_{ct}}{R_{ct(inh)}} \times 100 \quad (2)$$

where, $R_{ct(inh)}$ and R_{ct} are the values of charge transfer resistance in presence and absence of inhibitor in 3.5% NaCl respectively.

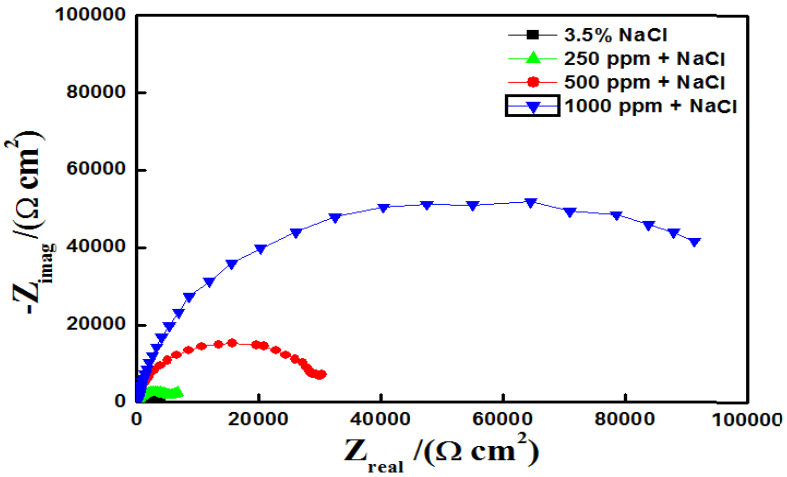

Figure 5. Nyquist plots for aluminium alloy in 3.5% NaCl without and with optimum concentrations of CCR extract.

At different concentrations CCR extract showed increase in value of R_{ct} with respect to blank 3.5% NaCl solution. The increase in R_{ct} values as shown in table 2 is attributed due to increase in resistance and adsorption of inhibitor molecules on aluminium alloy surface [37-40].

Table 2. Impedance parameters and inhibition efficiency values for aluminium alloy in 3.5% NaCl in absence and presence of CCR extract.

Solution	Conc.(ppm)	R_s (Ω cm^2)	R_{ct} (Ω cm^2)	η%
3.5% NaCl	-	2.0	4168	-
CCR Extract	250 ppm	2.0	6580	37
	500 ppm	1.7	23588	82
	1000 ppm	2.3	96080	96

3.2. Adsorption isotherm

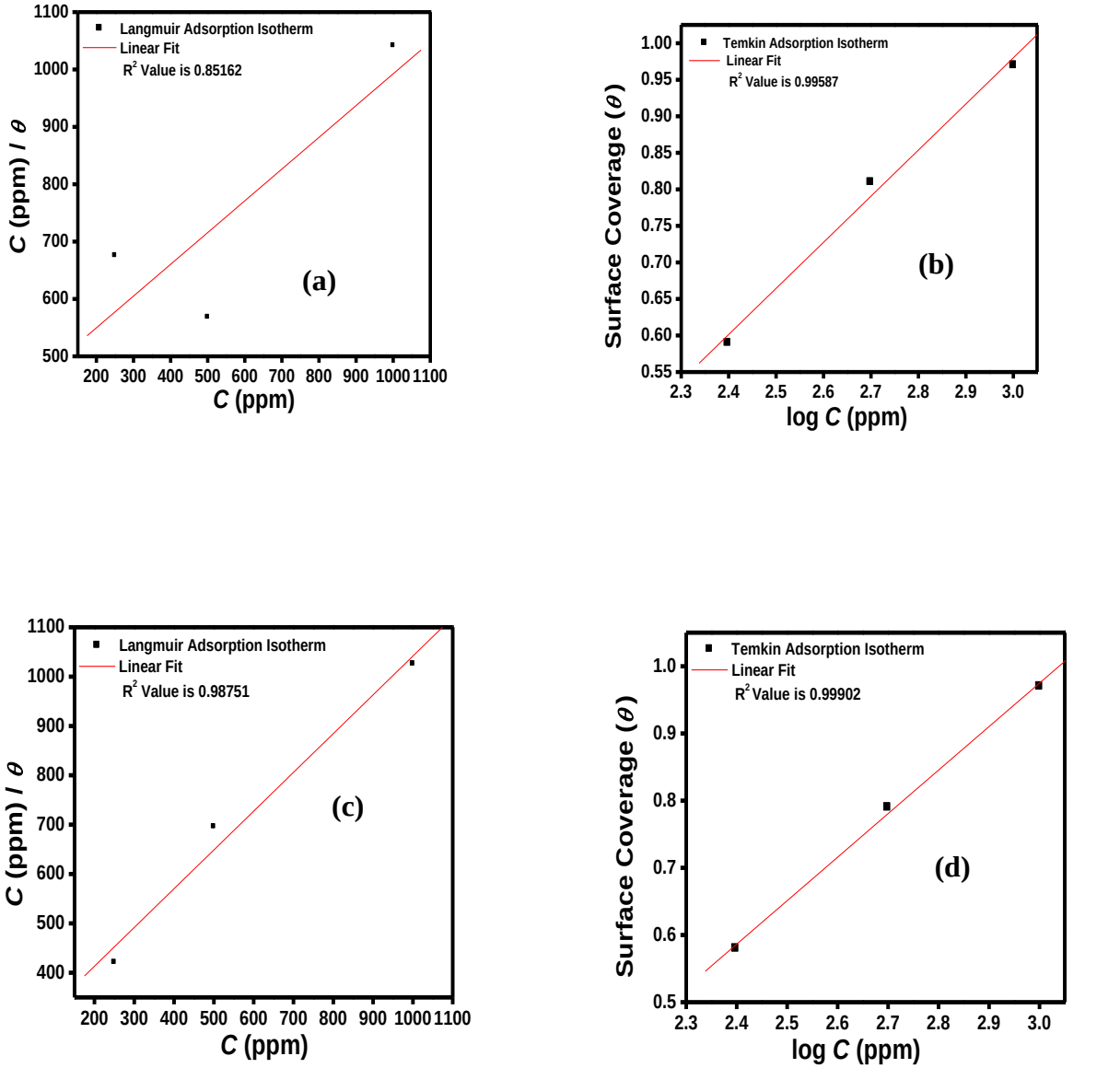

Figure 6. Langmuir and Temkin isotherms for adsorption of CCR extract on aluminium alloy surface in 3.5% NaCl (a) Electrochemical impedance spectroscopy (b) Tafel polarization.

The adsorption of an organic adsorbate on to metal-solution interface can be represented by a substitutional adsorption process between the organic molecules in the aqueous solution phase ($Org_{(sol)}$) and the water molecules on the metallic surface ($H_2O_{(ads)}$) [41].

$$Org_{(sol)} + xH_2O \rightarrow Org_{(ads)} + xH_2O_{(sol)} \quad (3)$$

where, x is the size ratio representing the number of water molecules replaced by one molecule of organic adsorbate. Basic information on the interaction between the inhibitor and the mild steel surface can be provided by the adsorption isotherm. It is essential to know the mode of adsorption and the adsorption isotherm that can give important information on the interaction of inhibitor and metal surface. Attempts were made to fit surface coverage values determined from electrochemical measurements into different adsorption isotherm models (figure 6a-d).

The linear regression coefficient values (R^2) determined from the plotted curves was found to be in the range of 0.99587 and 0.99902 for Temkin in EIS. And linear regression coefficient values (R^2) for Tafel polarization was 0.85162 and 0.98751 for Langmuir adsorption isotherm (equation 4). According to these results, it can be concluded that the best description of the adsorption behaviour of CCR extract can be best explained by Temkin adsorption isotherm given by equation 5.

$$\theta = \frac{bC_{inh}}{1+bC_{inh}} \quad \text{(Langmuir Isotherm)} \quad (4)$$

$$\exp(-2a\theta) = KC_{inh} \quad \text{(Temkin Isotherm)} \quad (5)$$

3.3. Surface Morphology Studies

3.3.1. Scanning Electrochemical Microscopy

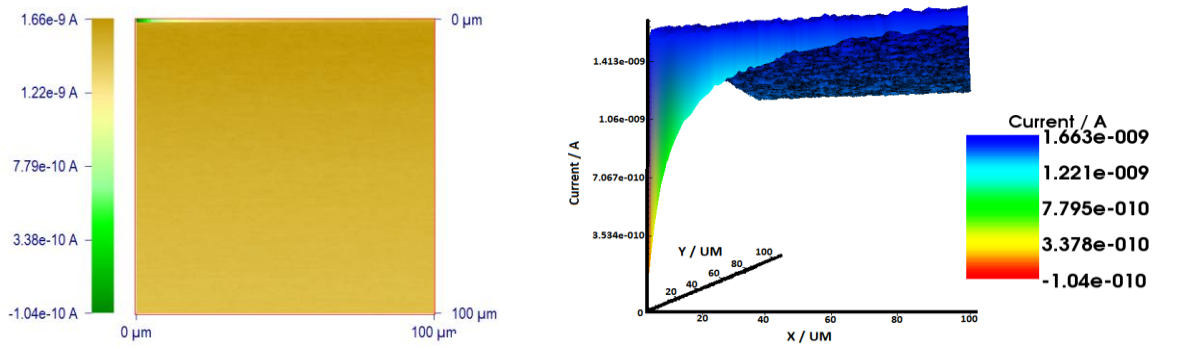

(a)

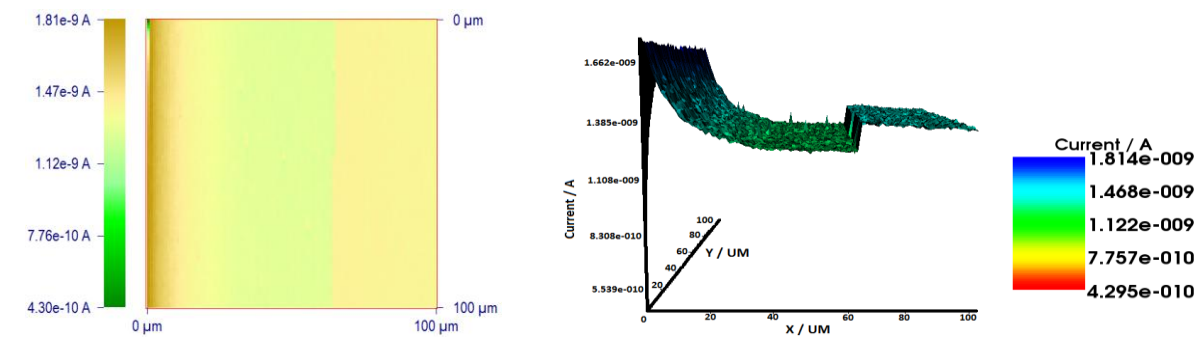

(b)

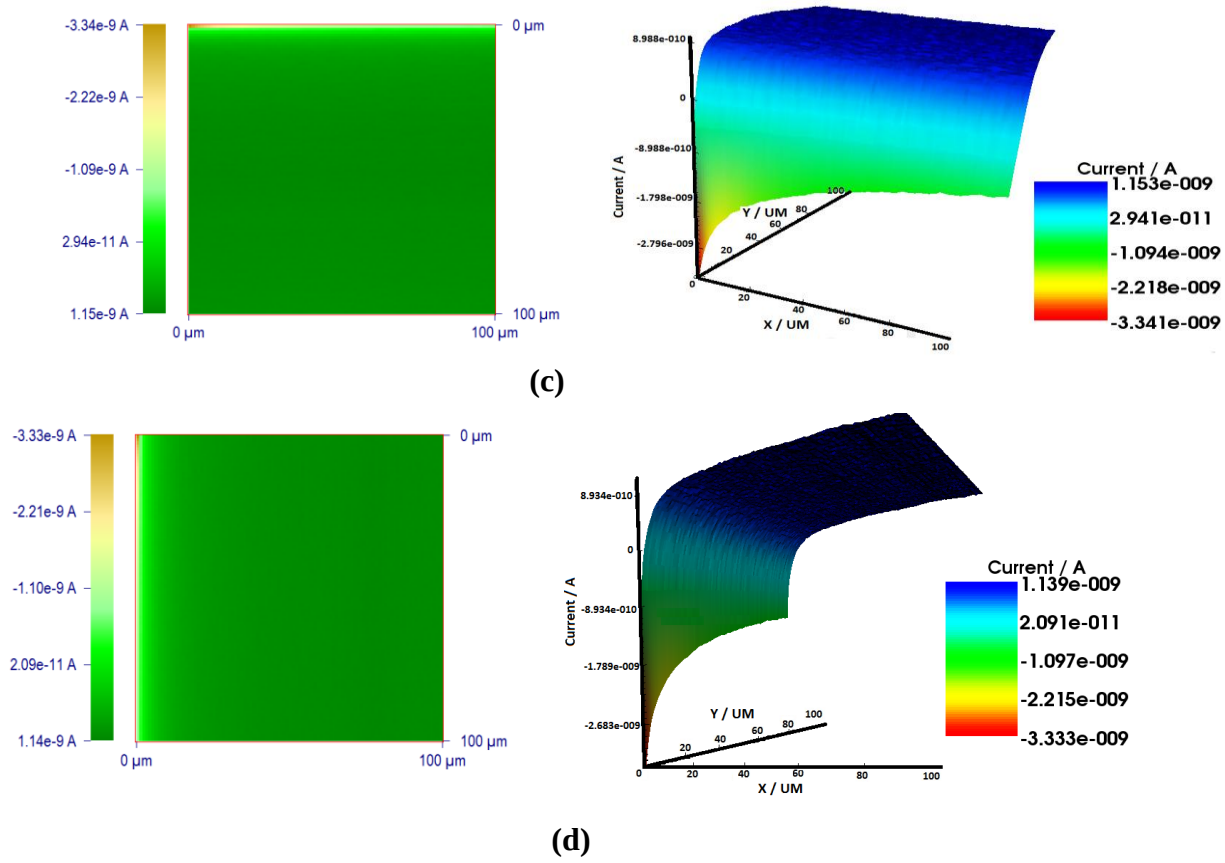

Figure 7. SECM images of (a) Blank 3.5% NaCl solution x axis, blank 3.5% NaCl solution x axis 3-D view (b) Blank 3.5% NaCl solution y axis, blank 3.5% NaCl solution y axis 3-D view (c) 1000 ppm CCR extract x axis, 1000 ppm CCR extract x axis 3-D view (d) 1000 ppm CCR extract y axis, 1000 ppm CCR extract y axis 3-D view.

The scanning electrochemical microscope (SECM) [42] has been introduced to the corrosion field, giving valuable microscopic information from a corroding surface [43, 44] allowing the measurement of local differences in electrochemical reactivity. The important advantage of the SECM technique is that it operates on both insulating (coated / films) and conducting (non-coated) surfaces, thus allowing one to easily distinguish between the coated and corroded surfaces [45, 46].

Figure 7a-d presents the morphology of the specimens visualized by scanning electrochemical microscope. Prior to each SECM scanning experiment; the tip-sample distance was established by approach curves performed above the insulating part of the coating at -0.70 V. The status of a corroded sample was studied by monitoring the probe (tip potential: 0.5 V *vs* Ag/AgCl/saturated KCl reference electrode) and the substrate (tip potential: -0.7 V) in test solutions. Corrosion activity is observed from 10 minutes after immersion in the electrolyte solution.

However, when an insulating surface (having film or coating) as we used CCR extract with 3.5% NaCl solution is approached in an SECM measurement the diffusion field surrounding the tip is hindered and the tip current decreases. This is typical for an insulating surface. On the contrary, an increase in the current is observed when a conductor blank 3.5% NaCl solution without CCR extract is approached, because the redox mediator is regenerated at the surface. In the absence of CCR extract

the aluminium alloy surface remains conductive, which are evidenced by an increase in current as the surface is approached. When CCR extract has been added to the solution a gradual transition from a conducting to an insulating surface is seen. Comparing the currents across the corroded sample and the specimens incorporated with inhibitor solution, the protection effect of the inhibitor adsorbed on the specimen surface can be justified [47, 48].

3.3.2. UV-Visible Spectroscopy

UV-Visible spectroscopy provides a strong evidence for the formation of a metal complex [49]. We obtained UV-Visible absorption spectra for optimum concentration of CCR extract before and after 3 hours immersion of aluminium alloy specimen. The electronic absorption spectrum of CCR extract before the aluminium alloy immersion shows two bands in UV-region as shown in figure 8. These bands may arise due to π-π* and n- π* transitions with a considerable charge transfer character.

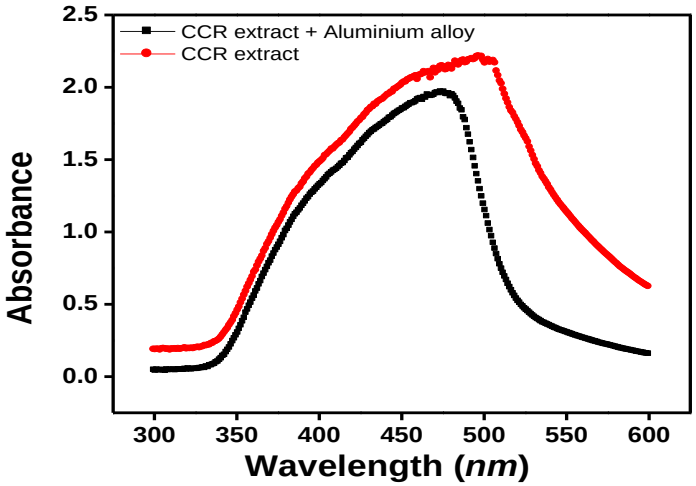

Figure 8. UV-Visible spectroscopy of CCR extract before and after 3 hours immersion of aluminum alloy.

After 3 hrs immersion of aluminium alloy sample change in the position of absorption maximum or change in the values of absorbance indicate the formation of a complex between two species in solution. However, there was no any significant change in the shape of the spectra.

4. MECHANISM OF ADSORPTION AND INHIBITION

The adsorption process is affected by the chemical structures of the inhibitors, the nature and charged surface of the metal and the distribution of charge over the whole inhibitor molecule [50]. Due to the complex nature of adsorption and inhibition of a given inhibitor, it is impossible for single adsorption mode between inhibitor and metal surface. Inhibitor molecules may be adsorbed on the metal surface in one or more of the following ways [51]:

(a) Electrostatic interaction between the charged molecules and the charged metal,

(b) Synergism due to different active constituents blocking the active sites of the metal

(c) Interaction of unshared electron pairs in the molecule with the metal,

(d) Interaction of p-electrons with the metal

The inhibition mechanism of the tested inhibitor is a combination of surface blockage and electrostatic repulsion between adsorbed surfactant layer and chloride ions. The inhibitor molecules containing hetero atoms (O, N, and S) with lone-pair electrons and aromatic rings set up their inhibition action via the adsorption of the inhibitor molecules on the metal surface.The increase in efficiency of inhibition of CCR extract indicates that the inhibitor molecules are adsorbed on the 7075 alloy surface with higher concentration, leading to greater surface coverage (θ) [52].

The inhibition process of 7075 alloy in the studied environment can be explained by the adsorption of the components of CCR extract on the metal surface. CCR extract contains berberine and other isoquinoline alkaloids. Active constituent molecules contain oxygen atoms in functional groups (O−H, C−H, C−O, and C=O), which meet the general consideration of typical corrosion inhibitors. The adsorption of these compounds on Al surface reduces the surface area that is available for the attack of the aggressive ion from the 3.5% NaCl solution. Studies have shown that alkaloids compounds can be used as corrosion inhibitors [53-56].

5. CONCLUSIONS

In this study, corrosion inhibition efficiency of CCR extract on 7075 aluminium alloy in 3.5% NaCl was determined by electrochemical and surface analysis. The potentiodynamic polarization data indicated that the CCR extract were of mixed type. Electrochemical impedance spectroscopy data reveals increase in R_{ct} values that accounted for good inhibition efficiency. The adsorption of the inhibitor molecules on the aluminium alloy surface was found to obey the Temkin adsorption isotherm. The surface studies by SECM, and UV-Visible Spectroscopy confirmed the blockage of metal surface through adsorption process. All these data support good inhibition tendency of CCR extract.

ACKNOWLEDGEMENTS

Authors are thankful to the post doctoral fellowship, financial assistance provided by the National Natural Science Foundation of China (No. 51274170) and the research grants from the Colonel Technology Fund of Southwest Petroleum University (Project No.2012XJZ013).

References

1. R. Rosliza, W. B. Wan Nik, S.Izman, Y.Prawoto, *Curr. Appl. Phys.* 10 (2010) 923.
2. H. Gerengi, *Ind. Eng. Chem. Res.* 51 (2012) 12835.
3. J. A. Hill, T. Markley, M. Forsyth, P. C. Howlett, B. R. Hinton, *J. Alloys Compd*. 509 (2011) 1683.
4. M. Dabala, E. Ramous, M. Magrini, *Mater. Corros.* 55 (2004) 381.

5. G. Bereket, A.Yurt, *Corros. Sci.* 43 (2001) 1179.
6. R. Rosliza, W. B. Wan Nik, H. B. Senin, *Mater. Chem. Phys.* 107 (2008) 281.
7. G. Bierwagen, R. Brown, D. Battocchi, S. Hayes, *Prog. Org. Coat.* 68 (2010) 48.
8. H. Gerengi, H. I. Sahin, *Ind. Eng. Chem. Res.* 51 (2012) 780.
9. O. K. Abiola , J. O. E. Otaigbe , O. J. Kio, *Corros. Sci.* 51 (2009) 1879.
10. M. A. Quraishi, A. Singh, V. K. Singh, D. K. Yadav, A. K. Singh, *Mater. Chem. Phys.* 122 (2010) 114.
11. A. Singh, I. Ahamad, V. K. Singh, M. A. Quraishi, *J. Solid State Electrochem.* 15 (2011) 1087.
12. A. Singh, Y. Lin, W. Liu, S. Yu, J. Pan, C. Ren, D. Kuanhai, *J. Ind. Eng. Chem.* (2014) http://dx.doi.org/10.1016/j.jiec.2014.01.033.
13. E. E. Oguzie, Kanayo L. Oguzie, Chris O. Akalezi, Irene O. Udeze, Jude N. Ogbulie, Victor O. Njoku, *Sustain. Chem. Eng.* 1 (2013) 214.
14. S. Kamath, Matthew Skeels, Aswini Pai, *Chin. Med.* 4 **(**2009) 17.
15. Q. Zhang, X. L. Piao, X. S. Piao, T. Lu, D. Wang, S. W. Kim, *Food chem. toxic*. (2011) doi:10.1016/j.fct.2010.09.032.
16. Yan Li, Peng Zhao, Qiang Liang , Baorong Hou, *Appl. Surf. Sci.* 252 (2005) 1245.
17. C. Ahn, J. Kor. Soc. *Cloth. Textil*. 33 (2009) 2002.
18. Allen J. Bard, Fu-Ren F. Fan, Juhyoun Kwak, Ovadia Lev, *Anal. Chem*. 61 (1989) 132.
19. Allen J. Bard, Guy Denuault, Chongmok Lee, Daniel Mandler, David O. Wipf, *Acc. Chem. Res*. 23 (1990) 357.
20. M. H. Delville, M. Tsionsky, A. J. Bard, *Langm.* 14 (1998) 2774.
21. A. Khamis, M. M. Saleh, M. I. Awad, *Corros. Sci*. 66 (2013) 343.
22. A. Singh, Y. Lin, W. Liu, D. Kuanhai, J. Pan, B. Huang, C. Ren, D. Zeng, *J. Taiwan Inst. Chem. Eng.* (2014) http://dx.doi.org/10.1016/j.jtice.2014.02.001.
23. I. Ahamad, R. Prasad, M. A. Quraishi, *Corros. Sci*. 52 (2010) 933.
24. Ambrish Singh, I. Ahamad, M. A. Quraishi, *Arab. J. Chem.* (2012) http:// doi.dx.10.1016/j.arabjc.2012.04.029.
25. D. K. Yadav, M. A. Quraishi, *Ind. Eng. Chem. Res*. 51 (2012) 8194.
26. A. Singh, I. Ahamad, V. K. Singh, M. A. Quraishi, *Chem. Eng. Comm*. 199 (2012) 63.
27. Ambrish Singh, M. A. Quraishi, *Res.Chem. Intermed.* (2013) doi: 10.1007/s11164-013-1398-3.
28. F. Bentiss, M. Lagrenee, *Mater. Environ. Sci*. 2 (2011) 13.
29. A. A. Hermas, M. S. Morad, M. H. J. Wahdan, *Appl. Electrochem*. 34 (2004) 95.
30. Ambrish Singh, I. Ahamad, V. K. Singh, M. A. Quraishi, *Chem. Engg. Comm.* 199 (2012) 63.
31. S. Safak, B. Duran, A. Yurt, G. Turkoglu, *Corros. Sci*. 54 (2012) 251.
32. H. Gerengi, K. Darowicki, P. Slepski, G. Bereket, J. Ryl, *J. Solid State Electrochem*. 14 (2010) 897.
33. F. Bentiss, M. Lebrini, M. Lagrenee, *Corros. Sci*. 47 (2005) 2915.
34. D. Asefi, M. Arami, N. M. Mahmoodi, *Corros. Sci*. 52 (2010) 794.
35. K.R. Ansari, M.A. Quraishi, Ambrish Singh, *Corros. Sci.* 79 (2014) 5.
36. X. Wang, H. Yang, F. Wang, *Corros. Sci*. 55 (2012) 145.
37. R. Solmaz, G. Kardas, M. Culha, B. Yazici, M. Erbil, *Electrochim. Acta* 53 (2008) 5941.
38. P. B. Raja, A. A. Rahim, H. Osman, K. Awang, *Int. J. Miner. Metall. Mater.* 18 (2011) 413.
39. A. Singh, J. N. Avyaya, Eno. E. Ebenso, M. A. Quraishi, Res. *Chem. Intermed.* 39 (2012) 537.
40. A. Singh, V. K. Singh, M. A. Quraishi, *Int. J. Corros.* doi:10.1155/2010/275983.
41. G. K. Gomma, M. H. Wahdan, *Mater. Chem. Phys*. 39 (1994) 142.
42. Z. Ding, Bernadette M. Quinn, Allen J. Bard, *J. Phys. Chem. B* 105 (2001) 6367.
43. R. M. Souto, Y. González-García, S. González, *Prog. Org. Coat*. 65 (2009) 435.
44. R. M. Souto, Y. González-García, J. Izquierdo, S. González, *Corros. Sci*. 52 (2010) 748.
45. Y. González-García, J. J. Santana, J. Gonzalez-Guzman, J. Izquierdo, S. González, R. M. Souto, *Prog. Org. Coat*. 69 (2010) 110.

46. K. Mansikkamaki, U. Haapanen, C. Johans, K. Kontturi, M. Valden, *J. Electrochem. Soc*. 153 (2006) B311.
47. J. Izquierdo, J. J. Santana, S. González, R. M. Souto, *Electrochim. Acta* 55 (2010) 8791.
48. A. T. Hubbard, F. C. Anson, Allen J. Bard, *Electroanal. Chem.* Marcel Dekker, New York; 4 1970 129.
49. W. H. Li, Q. He, S. T. Zhang, C. L. Pei, B. R. Hou, *J. Appl. Electrochem*. 38 (2008) 289.
50. A. Singh, T. Pramanik, A. Kumar, M. Gupta, *Asian J. Chem.* 25 (2013) 9808.
51. A. Singh, V. K. Singh, M. A. Quraishi, *Int. J. Corros.* (2010) http:// dx.doi:10.1155/2010/275983
52. K. F. Khaled, Mohamed N. H. Hamed, K. M. Abdel-Azim, N. S. Abdelshafi, *J. Solid State Electrochem*. 15 (2011) 663.
53. P. B. Raja, A. K. Qureshi, A. A. Rahim, H. Osman, K. Awang, *Corros. Sci*. 69 (2013) 292.
54. M. Lebrini, F. Robert, C. Roos, *Int. J. Electrochem. Sci*. 6 (2011) 847.
55. P. B. Raja, M. Fadaeinasab, A. K. Qureshi, A. A. Rahim, H. Osman, M. Litaudon, K. Awang, *Ind. Eng. Chem. Res*. 52 (2013) 10582.
56. A. Singh, Eno E. Ebenso, M. A. Quraishi, *Int. J. Corros.* (2012), http:// dx.doi.org/10.1155/2012/897430.